A

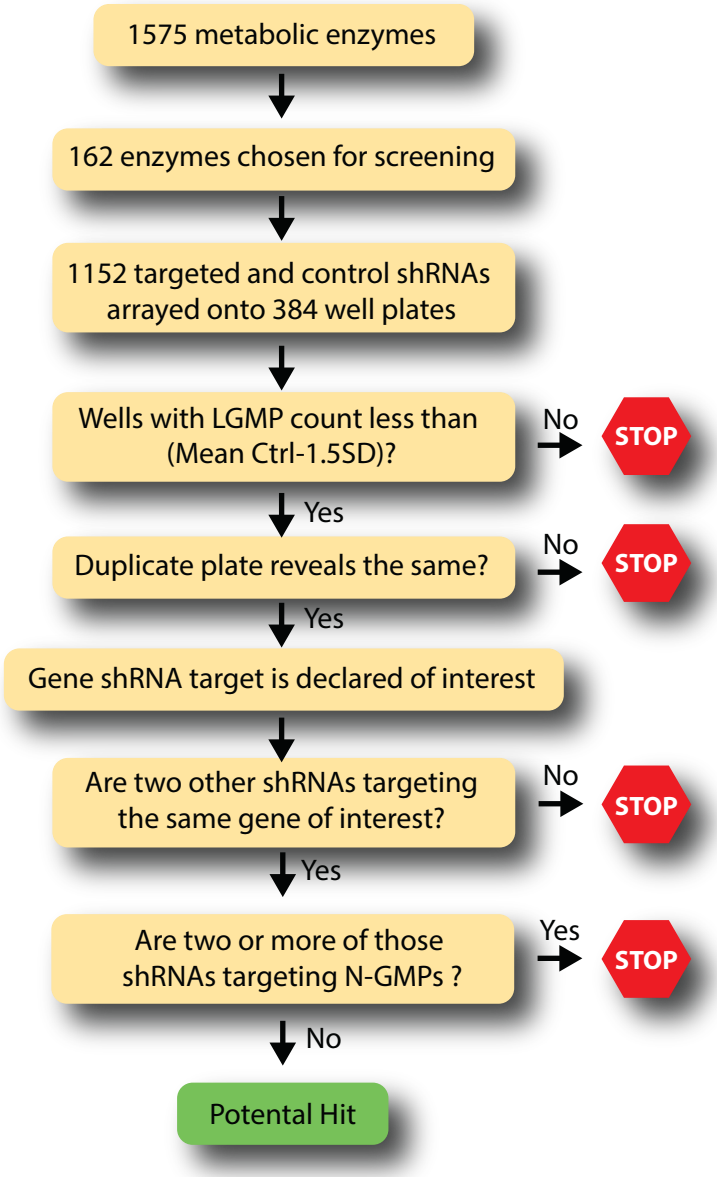

Yusuf RZ et al., Supp. Figure 1

A

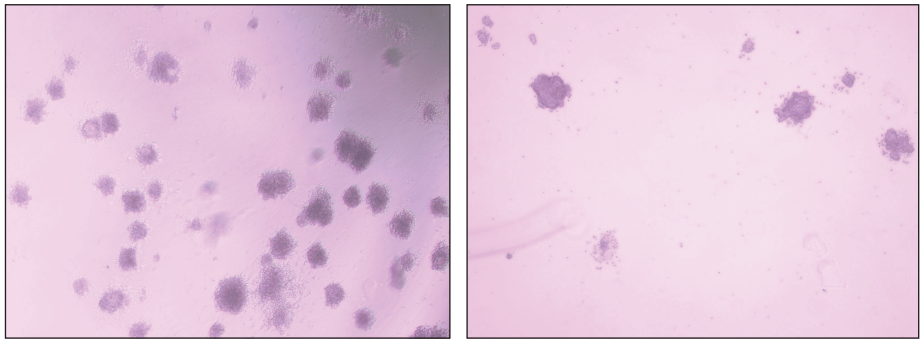

B

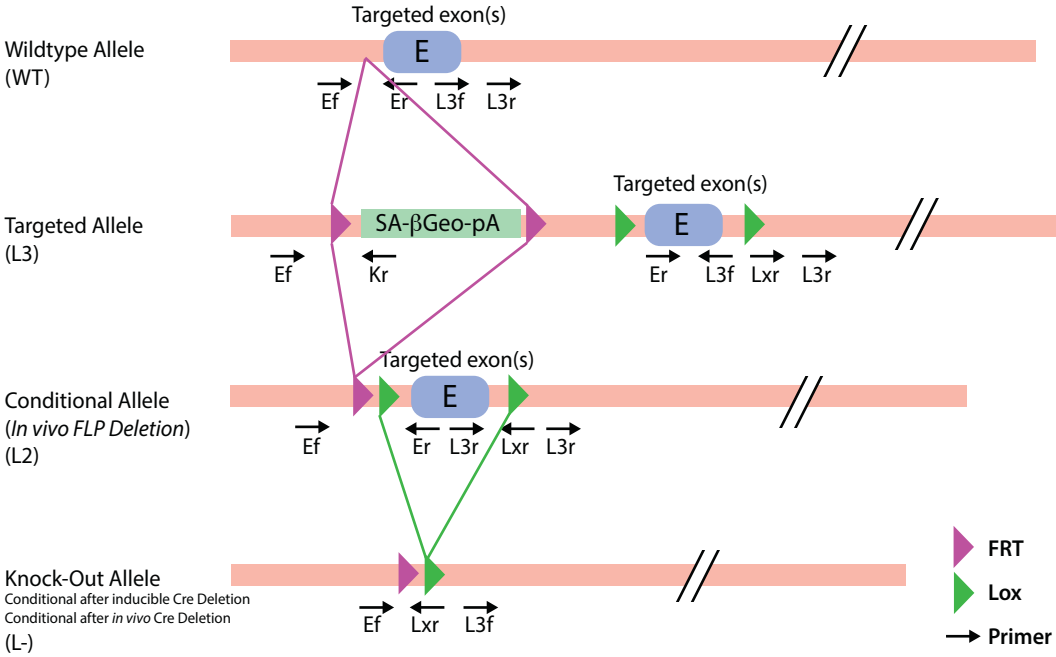

C

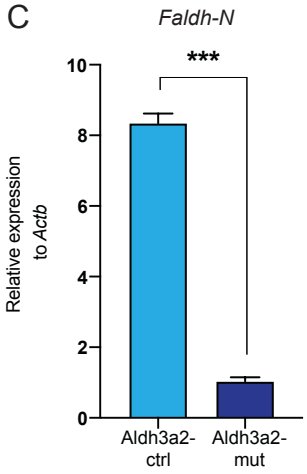

D

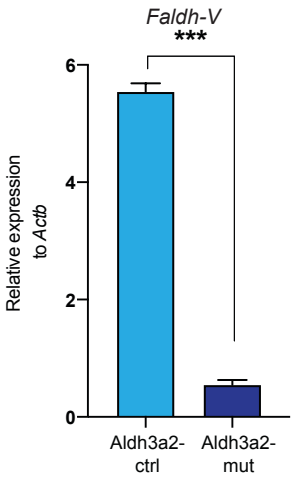

Yusuf RZ et al., Supp. Figure 2

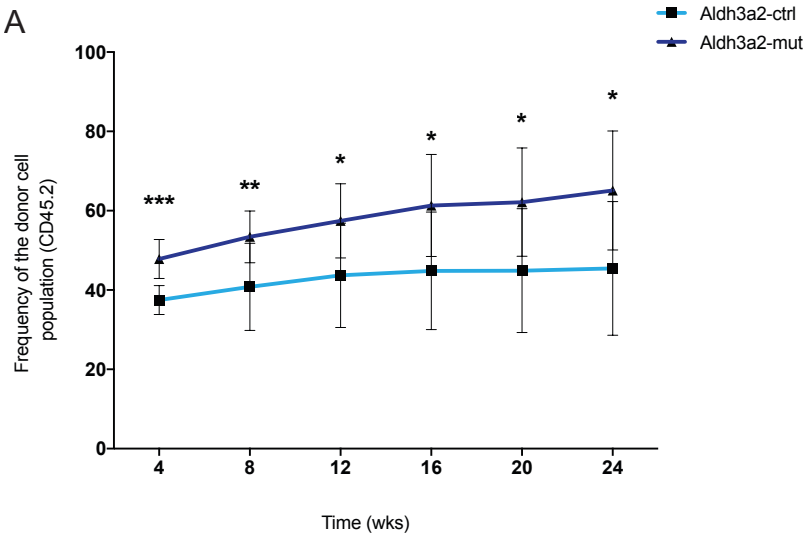

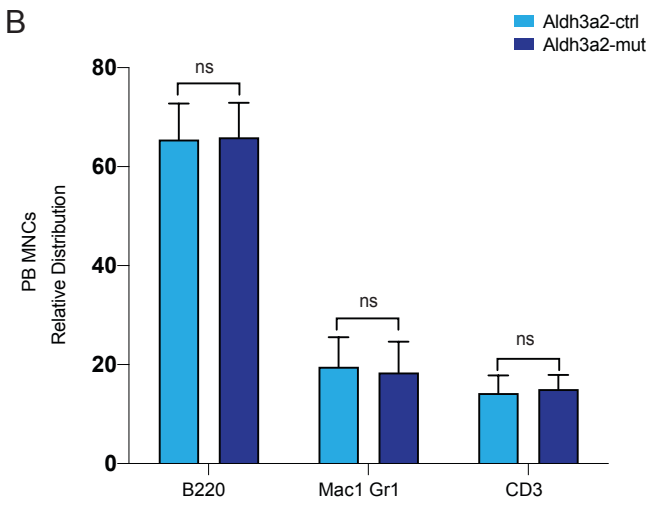

Yusuf RZ et al., Supp. Figure 3

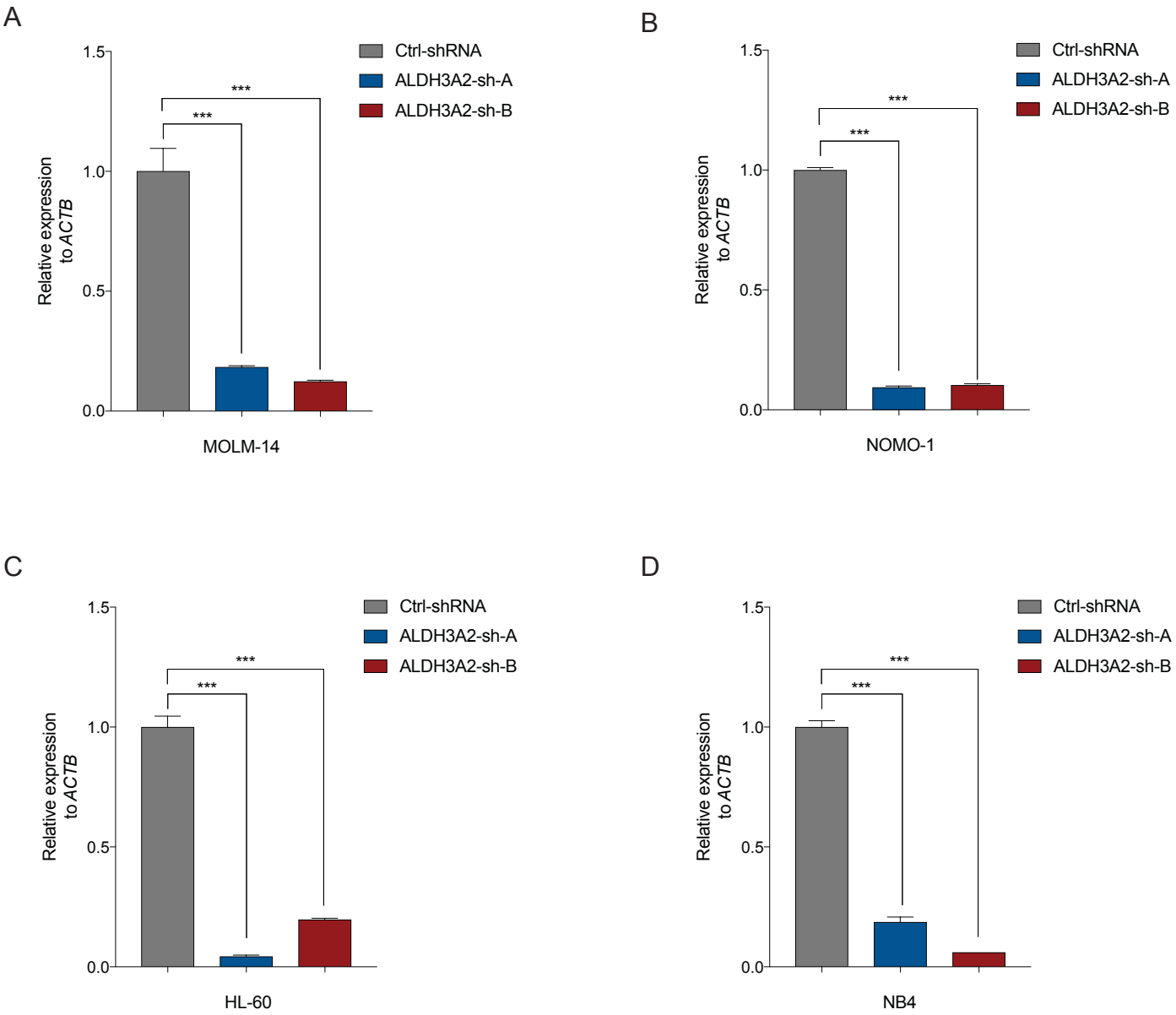

Yusuf RZ et al., Supp. Figure 4

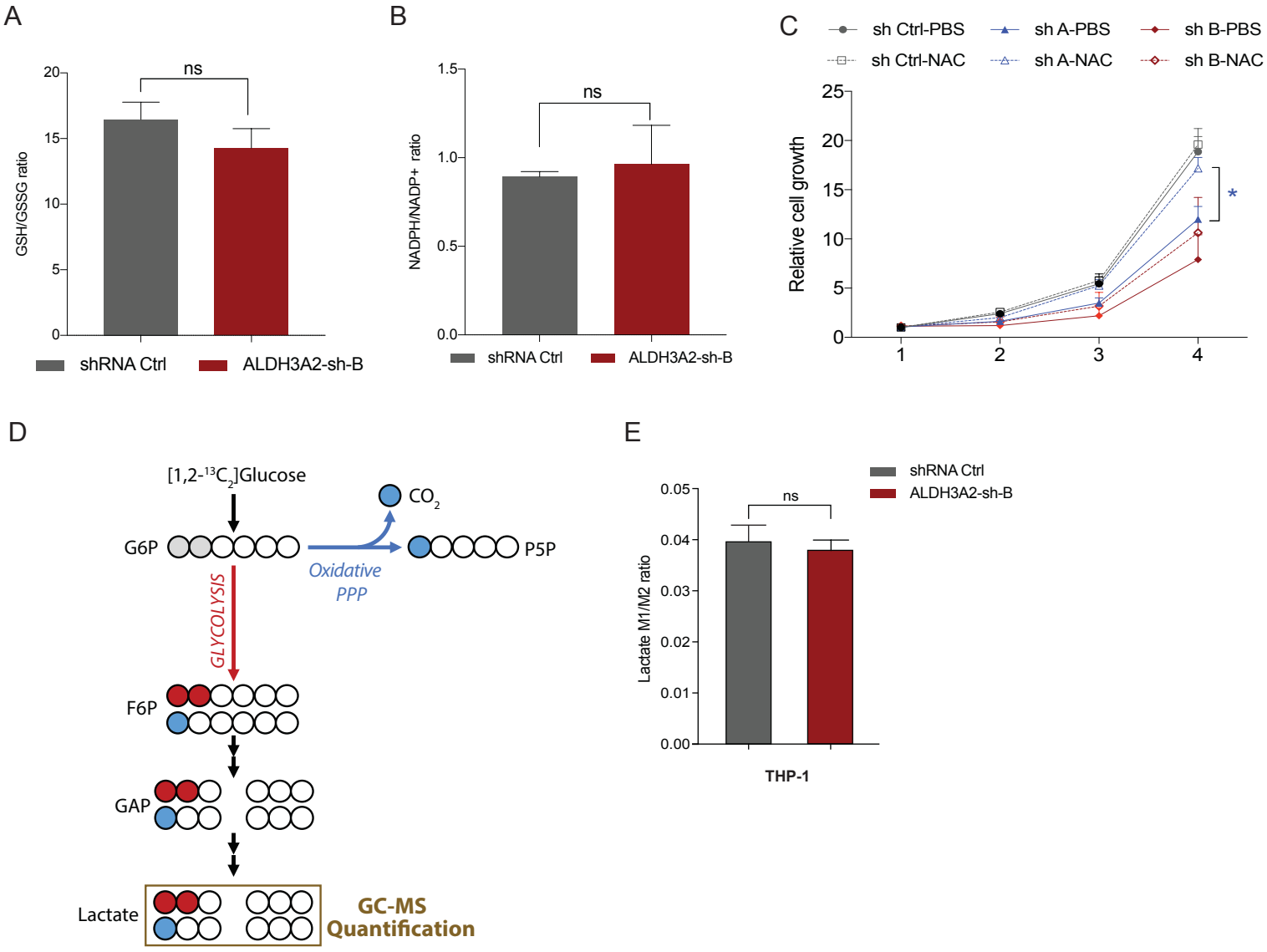

Yusuf RZ et al., Supp. Figure 5

A

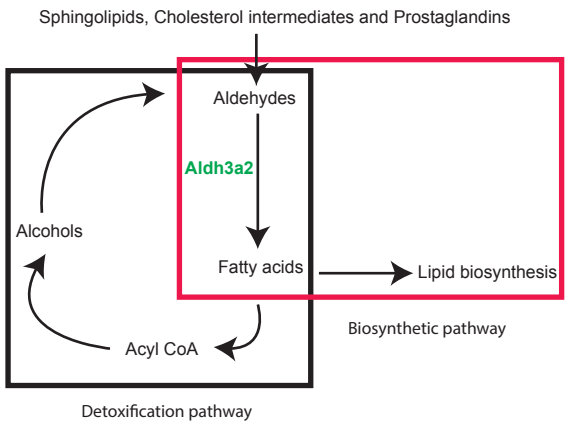

Yusuf RZ et al., Supp. Figure 6

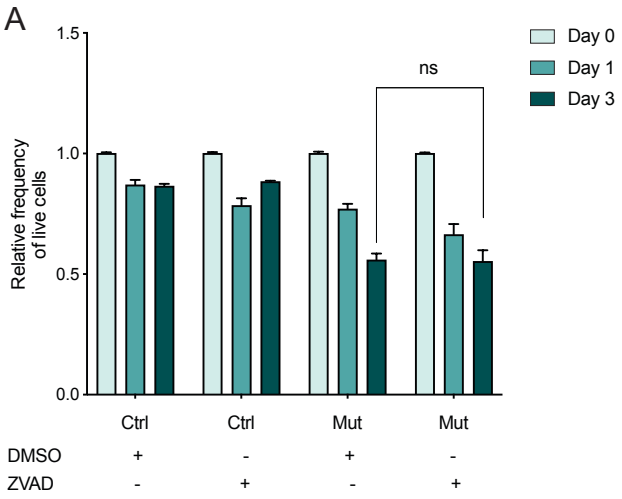

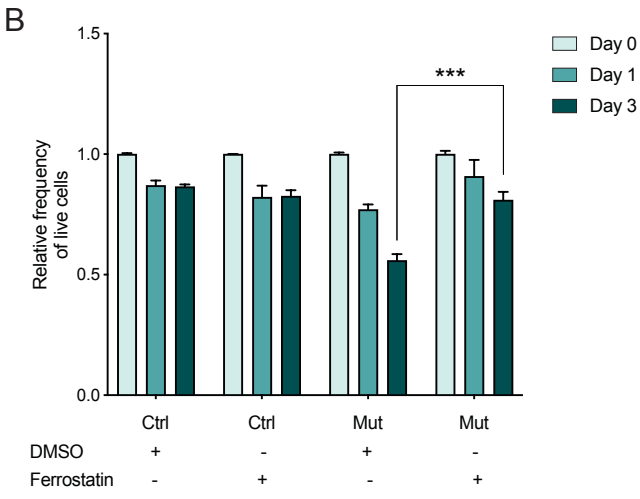

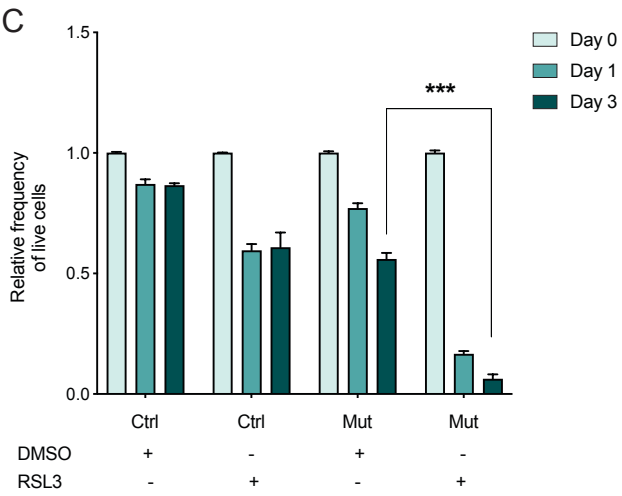

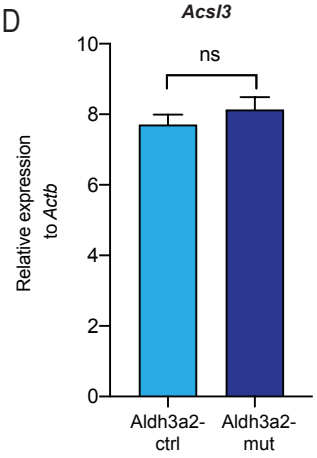

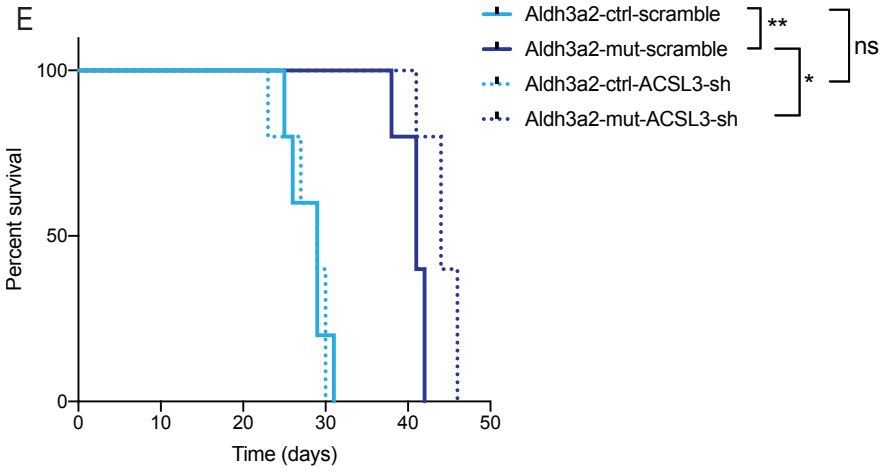

Yusuf RZ et al., Supp. Figure 7

Supplementary Materials and Methods

Generation of N-GMPs, L-GMPs and murine bone marrow stroma

L-GMPS: In order to generate L-GMPs six to eight-week old male mice carrying the DsRed fluorescent protein under the beta-actin promoter, henceforth referred to as DsRed mice, were treated with 5-flourouracil (5-FU) (Millipore Sigma). Single cell suspension of red blood cell-lysed bone marrow was infected with MSCV based retrovirus carrying the MLL-AF9 oncogene in tandem with a neomycin resistance gene (gift from Dr. Scott Armstrong) using polybrene (Millipore Sigma). After two rounds of infection, the infected cells were transplanted into lethally irradiated (9 Gy of irradiation from a ^{137}Cesium gamma source) C57BL/6J mice. These recipient mice designated "primary leukemic mice" became moribund at 8-12 weeks after transplant and were euthanized at the first signs of illness. Mononuclear bone marrow cells from these mice were transplanted into sub-lethally irradiated (4.5 Gy) C57BL/6J mice. These recipients, designated "secondary leukemic mice", became moribund at four weeks and were sacrificed at the first signs of illness. Mononuclear bone marrow from secondary leukemic mice was subjected to flow sorting in order to obtain DsRed positive L-GMPs according to the scheme of Kristov *et al*.[1]

NGMPs: N-GMPs were flow sorted from red blood cell lysed bone marrow from Ds-Red mice as described.[2]

Primary murine bone marrow stroma: Each batch of stroma was made from four actin-GFP mice. Mononuclear whole bone marrow was plated in alpha-MEM (Gibco) with 20 percent Fetal Bovine Serum (FBS) (Gibco) and 1 percent Penicillin Streptomycin (P/S) (ThermoFisher Scientific) for 28 days (media changes after 2, 14 and 28 days). Cells were selected for CD105^{+} cells using biotinylated CD105 antibody and Streptavidin magnetic beads (Dynabeads Biotin Binder, ThermoFisher Scientific) and columns and passaged four times. This fourth passage was maintained in media for 4 days, and these cells and their media was used for all experiments. The media in which these cells were maintained is referred to as "conditioned media".

Production of retroviruses and lentiviruses

The MLL-AF9 construct in an MSCV-neomycin vector was a gift from Dr. Scott Armstrong and retroviral production was carried out in HEK293-T cells (American Type Tissue Collection or ATCC) using the pCL-Eco plasmid (Addgene) and Fugene HD transfection reagent (Promega) according to the manufacturer's instructions.

Lentiviruses were made according to The Broad Institute protocol for shRNA/sgRNA/ORF low throughput viral production (10 cm dish/6 well plate) found here: https://portals.broadinstitute.org/gpp/public/resources/protocols.

Infection of L-GMPs and N-GMPs

Bone marrow mononuclear cells from 5 secondary leukemia mice (for L-GMPs) or 10 DsRed mice (for N-GMPs) were plated in transfection media which contained 10 ng/ml of Stem Cell Factor (SCF, Peprotech) 10 ng/ml of Interleukin 6 (IL-6, Peprotech) and 6 ng/ml of Interleukin 3 (IL-3, Peprotech) and infected with retrovirus using polybrene and spinfection (2 times, 24 hours apart). Cells were harvested 3 hours after spinfection.

RT-qPCR

RNA was extracted from cells using the RNeasy Micro Kit (Qiagen) and RT-PCR was performed using the SuperScript™ IV One-Step RT-PCR System according to the manufacturer's instructions. Taqman probes were used to perform qPCR for murine and human *Aldh3a2*.

Flow cytometry

The cocktail of antibodies staining for lineage antigens for N-GMPs consisted of biotin-labelled anti-mouse antibodies against, CD3e, CD4, CD8, CD19, B220, Gr-1, Mac-1 (from BD Biosciences) and CD127 antigens (from Biolegend). The cocktail of antibodies staining for lineage antigens for L-GMPs consisted of biotin-labelled anti-mouse antibodies against, CD3e, CD4, CD8, CD19, B220, Gr-1 (from BD Biosciences) and CD127 antigens (from Biolegend). Flow sorting was performed using the BD FACSAria

II. Analysis was performed using FlowJo Software (TreeStar Software). Secondary stains were performed as previously described.[1,3]

Proliferation was assessed by staining with a PE-conjugated mouse anti-Ki-67 antibody (BD Pharmingen; 1/10) and Hoechst 33342 (40µg/ml; Invitrogen) after fixation and permeabilization of the cells (BD Cytofix/Cytoperm Kit, BD Biosciences). Apoptosis was detected using active Caspase 3-PE (PE Active Caspase-3 Apoptosis Kit; BD Pharmingen) after fixation and permeabilization of the cells. Double-stranded DNA breaks and oxidative DNA damage were measured by staining respectively with an AlexaFluor 647-conjugated mouse anti-H2AX (pS139) antibody (BD Biosciences) and a FITC-conjugated mouse anti-8-OHdG antibody (Abcam) after fixation and permeabilization of the cells. Oxidative protein damage was detected by measuring protein carbonylation (FlowCellect Oxidative Stress Characterization Kit; Sigma-Aldrich). All stainings were performed according to the manufacturer's instructions.

Methylcellulose assays

Ten thousand N-GMPs or L-GMPs infected with lentiviruses expressing relevant shRNAs were added to 3 ml of methylcellulose (StemCell Technologies) plated per well of a 6 well plate. Number of cells were counted on day 7.

Metzeler Database Analysis

Raw CEL file data was downloaded from the Metzeler database[4] from GEO using the Bioconductor package, GEOquery[5] and processed using the 'affy' BioConductor package.[6] Arrays were quality-controlled with arrayQualityMetrics[7] and RMA normalized.[8] Median probe intensities for genes of interest were calculated and combined with survival data and subjected to survival analysis.

Estimation of oxidative pentose phosphate pathway activity

THP-1 cells transduced with lentivirus expressing Aldh3a2 shRNA B or Control shRNA were cultured in glucose-free Roswell Park Memorial Institute medium (RPMI, ThermoFisher Scientific) supplemented with 1 0mM [1,2-$^{13}C_2$]-glucose (Cambridge Isotope Laboratories) for 24 hours. Polar metabolites were isolated through methanol-

chloroform extraction and derivatized by a two-step process. First, 15 µl of methoxyamine in pyridine (MOX Reagent, Thermo Pierce) was added before incubation at 40˚C for 1.5 h. Next, 20 µl N-(tert-butyldimethylsilyl)-N-methyl-trifluoroacetamide, with 1% tert-Butyldimethylchlorosilane (TBDMS) (Sigma) was added, and samples were incubated at 60°C for 1 h. The reaction mixtures were quickly vortexed, centrifuged at 21,000 x g for 1 min, and supernatant was transferred to GC-MS vials for analysis.

Polar metabolites were analyzed on a 6890N GC with a DB-35ms Ultra Inert capillary column coupled to a 5975B Inert XL MS (Agilent). The flow rate of the helium carrier gas (Airgas) was maintained at 1 ml/min. The inlet temperature was held at 270°C. Injection volumes and split ratios ranged from 2 µl splitless to 1 µl with a 1:10 split, depending on sample concentration and detected ion abundances. Both scan and selected ion monitoring (SIM) modes were used to detect measured ions (with SIM parameters identical to previously published values.[9] The instrument was operated in electron ionization mode with an energy of 70 eV. For polar metabolite samples, the GC oven was first held at 100°C for 3 min, then ramped at 2.5°C/min to 300°C; masses were profiled from 150 to 625 amu when in scan mode. Raw abundance data was converted to mass isotopomer distributions (MIDs) and corrected for natural abundance using an in-house software operating in Matlab (MathWorks).[10] Activity of the oxidative pentose phosphate pathway was estimated by making the ratio of M+1 lactate over M+2 lactate as detailed in Supplementary Figure 5.

Supplementary References

1. Krivtsov AV, Twomey D, Feng Z, et al. Transformation from committed progenitor to leukaemia stem cell initiated by MLL-AF9. *Nature.* 2006;442(7104):818-822.
2. Akashi K, Traver D, Miyamoto T, Weissman IL. A clonogenic common myeloid progenitor that gives rise to all myeloid lineages. *Nature.* 2000;404(6774):193-197.
3. Saez B, Ferraro F, Yusuf RZ, et al. Inhibiting stromal cell heparan sulfate synthesis improves stem cell mobilization and enables engraftment without cytotoxic conditioning. *Blood.* 2014;124(19):2937-2947.

4. Metzeler KH, Hummel M, Bloomfield CD, et al. An 86-probe-set gene-expression signature predicts survival in cytogenetically normal acute myeloid leukemia. *Blood.* 2008;112(10):4193-4201.
5. Davis S, Meltzer PS. GEOquery: a bridge between the Gene Expression Omnibus (GEO) and BioConductor. *Bioinformatics.* 2007;23(14):1846-1847.
6. Gautier L, Cope L, Bolstad BM, Irizarry RA. affy--analysis of Affymetrix GeneChip data at the probe level. *Bioinformatics.* 2004;20(3):307-315.
7. Kauffmann A, Gentleman R, Huber W. arrayQualityMetrics--a bioconductor package for quality assessment of microarray data. *Bioinformatics.* 2009;25(3):415-416.
8. Irizarry RA, Bolstad BM, Collin F, Cope LM, Hobbs B, Speed TP. Summaries of Affymetrix GeneChip probe level data. *Nucleic Acids Res.* 2003;31(4):e15.
9. Ahn WS, Antoniewicz MR. Metabolic flux analysis of CHO cells at growth and non-growth phases using isotopic tracers and mass spectrometry. *Metab Eng.* 2011;13(5):598-609.
10. Fernandez CA, Des Rosiers C, Previs SF, David F, Brunengraber H. Correction of 13C mass isotopomer distributions for natural stable isotope abundance. *J Mass Spectrom.* 1996;31(3):255-262.

Supplementary Tables

Supplementary Table 1A: 117 rate limiting enzymes curated from classic texts

Gene name	Gene Symbol	Mouse gene ID
3-hydroxy-3-methylglutaryl-Coenzyme A reductase	Hmgcr	15357
6-phosphofructo-2-kinase/fructose-2,6-biphosphatase 1	Pfkfb1	18639
6-phosphofructo-2-kinase/fructose-2,6-biphosphatase 2	Pfkfb2	18640
6-phosphofructo-2-kinase/fructose-2,6-biphosphatase 3	Pfkfb3	170768
6-phosphofructo-2-kinase/fructose-2,6-biphosphatase 4	Pfkfb4	270198
Acetyl-Coenzyme A acyltransferase 2 (mitochondrial 3-oxoacyl-Coenzyme A thiolase)	Acaa2	52538
Acetyl-Coenzyme A carboxylase alpha	Acaca	107476
Acetyl-Coenzyme A carboxylase beta	Acacb	100705
Adenylosuccinate synthetase like 1	Adssl1	11565
Adenylosuccinate synthetase, non muscle	Adss	11566
ADP-dependent glucokinase	Adpgk	72141
Arginase type II	Arg2	11847
Arginase, liver	Arg1	11846
Argininosuccinate synthetase 1	Ass1	11898
ATP citrate lyase	Acly	104112
ATPase inhibitory factor 1	Atpif1	11983
Brain glycogen phosphorylase	Pygp	110078
Carbamoyl-phosphate synthetase 1	Cps1	227231
Carbamoyl-phosphate synthetase 2, aspartate transcarbamylase, and dihydroorotase	Cad	69719
Carnitine acetyl transferase	Crat	12908
Citrate lyase beta like	Clybl	69634

Citrate synthase	Cs	12974
Citrate synthase like	Csl	71832
Cytochrome c oxidase subunit IV isoform 1	Cox4i1	12857
Cytochrome c oxidase subunit IV isoform 2	Cox4i2	84682
Dihydrolipoamide S-acetyltransferase (E2 component of pyruvate dehydrogenase complex)	Dlat	235339
Enoyl-CoenzymeA, hydratase/3-hydroxyacyl coenzyme	Ehhadh	74147
Eph receptor B2	Ephb2	13844
Fructose bisphosphatase 1	Fbp1	14121
Fructose bisphosphatase 2	Fbp2	14120
fructose bisphosphatase 3	Fbp3	14122
Glucokinase	Gck	103988
Glucose 6 phosphatase, catalytic, 3	G6pc3	68401
Glucose 6-phosphatase, related sequence	G6pdrs	107634
glucose-6-phosphatase, catalytic	G6pc	14377
Glucose-6-phosphatase, catalytic, 2	G6pc2	14378
Glucose-6-phosphate dehydrogenase 2	G6pd2	14380
Glucose-6-phosphate dehydrogenase X-linked	G6pdx	14381
Glutamate-ammonia ligase (glutamine synthetase)	Glul	14645
Glutathione peroxidase 1	Gpx1	14775
Glutathione peroxidase 2	Gpx2	14776
Glutathione peroxidase 3	Gpx3	14778
Glutathione peroxidase 4	Gpx4	625249
Glutathione peroxidase 5	Gpx5	14780
Glutathione peroxidase 6	Gpx6	75512
Glutathione peroxidase 7	Gpx7	67305
Glutathione peroxidase 8	Gpx8	69590
Glycogen synthase1, muscle	Gys1	14936
Glycogen synthase 2	Gys2	232493
Hadha hydroxyacyl-Coenzyme A dehydrogenase/3-ketoacyl-Coenzyme A thiolase/enoyl-Coenzyme A hydratase (trifunctional protein), alpha subunit	Hadha	97212
Heme oxygenase (decycling) 1	Hmox1	15368
Heme oxygenase (decycling) 2	Hmox2	15369
Hexokinase 1	Hk1	15275
Hexokinase 2	Hk2	15277
Hexokinase 3	Hk3	212032
Hexokinase-1 related sequence 1	Hk1-rs1	110286
Hydroxyacyl-Coenzyme A dehydrogenase/3-ketoacyl-Coenzyme A thiolase/enoyl-Coenzyme A hydratase (trifunctional protein), beta subunit	Hadhb	231086
Inosine 5'-phosphate dehydrogenase 1	Impdh1	23917
Inosine 5'-phosphate dehydrogenase 2	Impdh2	23918
Isocitrate dehydrogenase 1 (NADP+), soluble	Idh1	15926
Isocitrate dehydrogenase 2 (NADP+), mitochondrial	Idh2	269951
Isocitrate dehydrogenase 3 (NAD+) alpha	Idh3a	67834
Isocitrate dehydrogenase 3 (NAD+) beta	Idh3b	170718
Isocitrate dehydrogenase 3 (NAD+), gamma	Idh3g	15929
Ketohexokinase	Khk	16548

Lactate dehydrogenase A	Ldha	16828
Lactate dehydrogenase A-like 6B	Ldhal6b	106557
Lactate dehydrogenase B	Ldhb	16832
Lactate dehydrogenase C	Ldhc	16833
Lactate dehydrogenase D	Ldhd	52815
Lens protein with glutamine synthetase domain	Lgsn	266744
Liver glycogen phosphorylase	Pygl	110095
Malic enzyme 1, NADP(+)-dependent, cytosolic	Me1	17436
Malic enzyme 2, NAD(+)-dependent, mitochondrial	Me2	107029
Malic enzyme 3, NADP(+)-dependent, mitochondrial	Me3	109264
Malic enzyme complex, mitochondrial	Mod2	110357
Malic enzyme, related sequence	Mod-rs	110087
Mitogen-activated protein kinase 1	Mapk1	26413
Mitogen-activated protein 2 kinase 2	Map2k2	26396
Mitogen-activated protein 2 kinase 5	Map2k5	23938
mitogen-activated protein 2 kinase 2	Map3k2	26405
MLX interacting protein-like	Mlxipl	58805
Muscle glycogen phosphorylase	Pygm	19309
N-acetylglutamate synthase	Nags	217214
Ornithine transcarbamylase	Otc	18416
Oxoglutarate dehydrogenase (lipoamide)	Ogdh	18293
Phosphoenolpyruvate carboxykinase 1, cytosolic	Pck1	18534
Phosphoenolpyruvate carboxykinase 2	Pck2	74551
Phosphofructokinase, liver, B-type	Pfkl	18641
Phosphofructokinase, muscle	Pfkm	18642
Phosphofructokinase, platelet	Pfkp	56421
Phosphofructokinase, polypeptide X	Pfkx	18642
Phosphogluconate dehydrogenase	Pgd	110208
Phosphoribosyl pyrophosphate amidotransferase	Ppat	231327
Phosphoribosyl pyrophosphate synthetase 1	Prps1	19139
Phosphoribosyl pyrophosphate synthetase 1-like 1	Prps1l1	75456
Phosphoribosyl pyrophosphate synthetase 2	Prps2	110639
Phosphoribosyl pyrophosphate synthetase-associated protein 1	Prpsap1	67763
Protein kinase, cAMP dependent regulatory, type I	Prkar1b	19085
Protein kinase, cAMP dependent regulatory, type I, alpha	Prkar1a	19084
Protein kinase, cAMP dependent regulatory, type II alpha	Prkar2a	19087
Protein kinase, cAMP dependent regulatory, type II beta	Prkar2b	19088
Protein kinase, cAMP dependent, catalytic, alpha	Prkaca	18747
Protein kinase, cAMP dependent, catalytic, beta	Prkacb	18749
Pyruvate carboxylase	Pcx	18563
Pyruvate dehydrogenase (lipoamide) beta	Pdhb	68263
Pyruvate dehydrogenase complex, component X	Pdhx	27402
Pyruvate dehydrogenase E1 alpha 1	Pdha1	18597
Pyruvate dehydrogenase E1 alpha 2	Pdha2	18598
Pyruvate kinase liver and red blood cell	Pklr	18770
Pyruvate kinase, muscle	Pkm2	18746
Ribonucleotide reductase M1	Rrm1	20133
Ribonucleotide reductase M1, related sequence 13	Rrm1-rs13	110820
Ribonucleotide reductase M2	Rrm2	20135

Ribonucleotide reductase M2 B	Rrm2b	382985
Solute carrier family 25 (mitochondrial carnitine/acylcarnitine translocase), member 20	Slc25a20	57279
UDP-glucose pyrophosphorylase 2	Ugp2	216558

Supplementary Table 1B: Genes over-expressed in L-GMPs versus N-GMPs (from Krivstov *et al.*[1])

Gene name	Gene Symbol	Mouse gene ID
AcylcoA dehydrogenase 11	Acad11	11370
Lysosomal; acid phosphatase 2	Acp2	11432
Aldehyde dehydrogenase family 3, member A2	Aldh3a2	11671
Aldehyde dehydrogenase family 3, member B1	Aldh3b1	67689
aldolase C fructose bisphosphate	Aldoc	11676
adenosine monophosphate deaminase 3	Ampd3	11717
Aspartocyclase	Aspa	11484
ATPase, H+ transporting, lysosomal V1 subunit E1	ATP6v1e1	11973
UDP-GlcNAc:betaGal beta-1,3-N-acetylglucosaminyltransferase 8	B3gnt8	232984
Beta-1,4-N-acetyl-galactosaminyl transferase 1	B4galnt1	14421
Biliverdin reductase B (flavin reductase (NADPH))	Blvrb	233016
CDP-diacylglycerol synthase (phosphatidate cytidylyltransferase) 2	Cds2	110911
Creatine kinase, muscle	Ckm	12715
Cytochrome b-245, alpha polypeptide	Cyba	13057
Cytochrome P450, family 4, subfamily f, polypeptide 18	Cyp4f18	72054
Dicarbonyl L-xylulose reductase	Dcxr	67880
Diacylglycerol O-acyltransferase 1	Dgat1	13350
Diacylglycerol kinase, gamma	Dgkg	110197
Dehydrogenase/reductase (SDR family) member 1	Dhrs1	52585
Ectonucleoside triphosphate diphosphohydrolase 1	Entpd1	12495
Ferrochelatase	Fech	14151
Flavin containing monooxygenase 5	Fmo5	14263
Guanine deaminase	Gda	14544
Glucosamine (N-acetyl)-6-sulfatase	Gns	75612
Glutathione peroxidase 3	Gpx3	14778
Glutathione reductase	Gsr	14782
Hydroxyprostaglandin dehydrogenase 15 (NAD)	Hpgd	15446
Indolethylamine N-methyltransferase	Inmt	21743
Ketohexokinase	Khk	16548
Monoglyceride lipase	Mgll	23945
Monoacylglycerol O-acyltransferase 2	Mogat2	233549
Neuraminidase 1	Neu1	18010
Phosphodiesterase 1B, Ca2+-calmodulin dependent	Pde1b	18574
Phosphodiesterase 3A, cGMP inhibited	Pde3a	54611
Phosphodiesterase 8A	Pde8a	18584
Phosphogluconate dehydrogenase	Pgd	110208
Phospholipase C, beta 2	Plcb2	18796

Procollagen-lysine, 2-oxoglutarate 5-dioxygenase 1	Plod1	18822
Phosphomannomutase 2	Pmm	54128
Paraoxonase 3	Pon3	269823
Phosphatidylserine synthase 2	Ptdss2	27388
Liver glycogen phosphorylase	Pygl	110095
Spermidine/spermine N1-acetyltransferase 1	Sat1	20229
Solute carrier family 25 (mitochondrial carrier, phosphate carrier), member 25	Slc25a25	227731
UDP-glucose pyrophosphorylase 2	Ugp2	216558

Supplementary Figure Legends

Supplementary Figure 1. ***Metabolism-focused screen in L-GMPs and N-GMPs.*** Filters and algorithm applied to the shRNA screen.

Supplementary Figure 2. ***Models used to investigate Aldh3a2 depletion in vitro and in vivo.*** **A)** Representative images of a methylcellulose assay showing colony number and morphology in *Aldh3a2* depleted and control L-GMPs. **B)** Schema for generating Aldh3a2$^{fl/fl}$ mice. **C)** qPCR results showing expression of Aldh3a2 (FALDH) splice variants V and N in Aldh3a2-control and mutant leukemic cells, relative to beta-actin (*Actb*).

Supplementary Figure 3. ***Aldh3a2 depletion favors normal hematopoiesis in a conditional mouse model.*** **A)** Relative peripheral blood (PB) reconstitution after transplantation of recipient B6.SJL (CD45.1) mice transfused with whole BM cells from Aldh3a2-control or mutant mice (CD45.2^{+}) competed with equal numbers of wild-type CD45.1 whole BM cells (n=10 and 9 recipients per group respectively). **B)** Contribution of Aldh3a2-control and mutant HSPCs to peripheral blood B cells (B220), myeloid cells (Mac1, Gr1) and T cells (CD3) 24 weeks after transplantation (n=10 and 9 recipients per group respectively).

Supplementary Figure 4. ***Aldh3a2 depletion in human AML cell lines with shRNA.*** **A-D)** Effective knockdown of *ALDH3A2* expression in MOLM-14 (A), NOMO-1 (B), HL-60 (C) and NB4 cells (D) with two independent shRNAs (ALDH3A2-sh-A and ALDH3A2-sh-B) compared to control shRNA. Data are representative of at least 2 independent experiments; n=3 replicates per cell line per experiment. Data are represented as mean +/- SD. ^{ns}P>.05; *P<.05; **P<.01; ***P<.001

Supplementary Figure 5. ***Antioxidant response in ALDH3A2-depleted human AML cells.*** **A)** Ratio of oxidized to reduced glutathione in *ALDH3A2*-depleted THP-1 cells. **B)** Ratio of NADPH/NADP^{+} in *ALDH3A2*-depleted THP-1 cells. **C)** Growth kinetics of *ALDH3A2*-depleted THP-1 cells treated with N-Acetyl-Cysteine (NAC). **D)** Schema

showing that in cells cultured in [1,2-$^{13}C_2$]-glucose medium, the oxidative pentose phosphate pathway (PPP) generates single ^{13}C-labeled (M1) intermediates and glycolysis generates double ^{13}C-labeled (M2) intermediates. **E)** Lactate M1/M2 ratio in *ALDH3A2*-depleted THP-1 cells. Data are representative of at least 2 independent experiments; n=3 replicates per cell line per experiment. Data are represented as mean +/- SD. ^{ns}P>.05; *P<.05; **P<.01; ***P<.001.

Supplementary Figure 6. ***Metabolic role of Aldh3a2.*** **A)** The fatty acid alcohol cycle depicting the role of Aldh3a2 in converting alcohols and aldehydes to fatty acids. Depletion of the enzyme can lead to a depletion of fatty acids and accumulation of alcohols and aldehydes.

Supplementary Figure 7: ***Role of ferroptosis and apoptosis in Aldh3a2-depleted leukemia phenotype.*** **A-C)** Frequency of live Aldh3a2-control and mutant LSPCs over three days of culture and treatment with vehicle (DMSO), ZVAD (A), Ferrostatin (B) and RSL3 (C). A snapshot of this data (for day 3) is also presented in main Figure 7D, E and F. **D)** qPCR results showing *Acsl3* expression in Aldh3a2-control and mutant leukemia cells, relative to beta-actin (*Actb*). **E)** Sublethally irradiated C57BL/6J mice were injected with Aldh3a2-control and mutant leukemia cells, from primary leukemic mice, infected with lentivirus expressing *Acsl3* or scrambled shRNA. Forty eight hours after injection mice were injected with 3 doses of Poly(I):Poly(C) on alternate days and leukemia development was monitored. Kaplan-Meier survival curve of animals that developed leukemia is shown. n=3 replicates per cell line per experiment. Data are represented as mean +/- SD. ^{ns}P>.05; *P<.05; **P<.01; ***P<.001.